Gene Expression The Journal of Liver Research, Vol. 19, pp. 199–214
1052-2166/19 $90.00 + .00
DOI: https://doi.org/10.3727/105221619X15638857793317
E-ISSN 1555-3884
www.cognizantcommunication.com

Long-Term Engineered Cultures of Primary Mouse Hepatocytes for Strain and Species Comparison Studies During Drug Development

Brenton R. Ware,*†[1] Grace E. Brown,†[1] Valerie Y. Soldatow,‡ Edward L. LeCluyse,‡ and Salman R. Khetani*†§

*School of Biomedical Engineering, Colorado State University, Fort Collins, CO, USA
†Department of Bioengineering, University of Illinois at Chicago, Chicago, IL, USA
‡The Hamner Institutes for Health Sciences, Research Triangle Park, NC, USA
§Department of Mechanical Engineering, Colorado State University, Fort Collins, CO, USA

Testing drugs in isogenic rodent strains to satisfy regulatory requirements is insufficient for derisking organ toxicity in genetically diverse human populations; in contrast, advances in mouse genetics can help mitigate these limitations. Compared to the expensive and slower in vivo testing, in vitro cultures enable the testing of large compound libraries toward prioritizing lead compounds and selecting an animal model with human-like response to a compound. In the case of the liver, a leading cause of drug attrition, isolated primary mouse hepatocytes (PMHs) rapidly decline in function within current culture platforms, which restricts their use for assessing the effects of longer-term compound exposure. Here we addressed this challenge by fabricating mouse micropatterned cocultures (mMPCC) containing PMHs and 3T3-J2 murine embryonic fibroblasts that displayed 4 weeks of functions; mMPCCs created from either C57Bl/6J or CD-1 PMHs outperformed collagen/Matrigel™ sandwich-cultured hepatocyte monocultures by ~143-fold, 413-fold, and 10-fold for albumin secretion, urea synthesis, and cytochrome P450 activities, respectively. Such functional longevity of mMPCCs enabled in vivo relevant comparisons across strains for CYP induction and hepatotoxicity following exposure to 14 compounds with subsequent comparison to responses in primary human hepatocytes (PHHs). In conclusion, mMPCCs display high levels of major liver functions for several weeks and can be used to assess strain- and species-specific compound effects when used in conjunction with responses in PHHs. Ultimately, mMPCCs can be used to leverage the power of mouse genetics for characterizing subpopulations sensitive to compounds, characterizing the degree of interindividual variability, and elucidating genetic determinants of severe hepatotoxicity in humans.

Key words: Micropatterned cocultures; Drug-induced liver injury; Murine embryonic fibroblasts; Cytochrome P450; Sandwich cultures

INTRODUCTION

Testing compounds in isogenic strains of rodents during preclinical screening, and later in small human cohorts in phase I/II clinical trials, is insufficient for derisking organ toxicity in genetically diverse human populations across many drug classes[1,2]. In contrast, recent advances in mouse genetics (e.g., Collaborative Cross) have proven to be highly useful in identifying subpopulations sensitive to compounds, characterizing the degree of interindividual variability, and providing genetic evidence for toxicity mechanisms[3]. Thus, when coupled with human-relevant assays to determine any species-specific differences in the metabolism of certain compounds, genetically diverse mouse strains represent a promising model for the preclinical safety screening of drugs and industrial chemicals.

Owing to their high cost and slow turnaround, in vivo animal studies are most suitable for testing a small number of compounds during the later stages of preclinical development. In contrast, faster and cheaper in vitro assays/models can be used on many compounds at all stages of safety evaluation and combined with structure–activity relationship (SAR) optimization to select promising lead compounds for the in vivo testing required by regulatory agencies. Since toxicity to the liver is a leading cause of compound attrition and acute liver failure[4],

[1]These authors provided equal contribution to this work.
Address correspondence to Salman R. Khetani, Ph.D., Department of Bioengineering, University of Illinois at Chicago, 851 S Morgan St, 218 SEO, Chicago, IL 60607, USA. Tel: 312-413-9424; Fax: 312-996-5921; E-mail: skhetani@uic.edu

in vitro liver models play an important role during compound development. Primary hepatocytes are ideal for constructing such models given their physiological relevance as opposed to transformed immortalized cell lines[5]. However, primary mouse hepatocytes (PMHs) display a rapid decline in phenotypic functions and sensitivity to compounds when cultured on conventional collagen-adsorbed plastic[6]. Sandwiching PMHs between two layers of gelled extracellular matrix (ECM) proteins (e.g., collagen and Matrigel™) can enhance gene expression and functions over adsorbed collagen controls; however, hepatocyte integrity and functions still decline within days of culture initiation[7–9]. Even more advanced matrices for cell seeding, such as poly[*N*-*p*-vinylbenzyl-4-*O*- -D-galactopyranosyl-D-gluconamide] with E-cadherin-Fc[10] and polyacrylamide gels of in vivo-like stiffness[11], cannot rescue the PMH phenotype beyond a few days. Providing higher oxygen tensions to PMHs using specialized substrates increases albumin production, but such production still declines within 4 days[12]. Last, three-dimensional (3D) spheroids/clusters of PMHs lose their prototypical morphology over 6 days, while it is not clear if functions are maintained beyond 2 days of culture[13]. Therefore, there remains a need to develop a culture platform that can maintain the drug metabolism capacity of PMH cultures for several weeks to enable longer-term exposures to compounds and their metabolites as in vivo.

Coculture with both liver- and non-liver-derived non-parenchymal (NPC) types can modulate hepatic functions in both liver development and physiology[14]. Specifically, liver formation from the endodermal foregut and mesenchymal vascular structures in the embryo is mediated by heterotypic interactions with other cell types[14]; without interaction with the mesenchyme, the endoderm does not undergo complete hepatic differentiation[15,16]. Some of these interactions can be replicated in vitro by coculturing primary hepatocytes from different species with NPCs derived from multiple species and tissues, such as rat hepatocytes cocultured with either C3H/10T1/2 mouse embryo cells[17], 3T3 murine embryonic fibroblasts[14], or human fibroblasts[18]. For PMHs, only a handful of studies have utilized coculture with NPC types. Specifically, coculture with liver epithelial cells was shown to improve albumin and cytochrome-P450 3A (CYP3A) gene expression in PMHs over 6 days relative to monocultures; however, functional endpoints were lacking[19]. Similarly, PMHs displayed higher proliferation over 2 days when cocultured with the whole NPC fraction of the mouse liver, but CYP enzyme activities were not measured[20]. Therefore, there remains a need to design an optimal coculture microenvironment for PMHs toward maintaining drug-metabolizing capacity for several weeks.

3T3-J2 murine embryonic fibroblasts are known to express molecules present in the liver (e.g., decorin, VEGF, T-cadherin) at higher levels than other 3T3 subclones (e.g., 3T3-NIH, 3T3-Swiss, 3T3-L1) and primary mouse embryonic fibroblasts[21,22]. Such high expression of liver-like molecules allows the 3T3-J2 fibroblasts to stabilize the phenotypic functions of primary rat[14] and primary human hepatocytes (PHHs)[23] for 4+ weeks within a micropatterned coculture (MPCC) format with empirically optimized dimensions; contact between the two cell types is required for stabilization of hepatic functions as fibroblast-conditioned medium alone does not suffice for stabilizing hepatic functions[24]. Furthermore, 3T3-J2 fibroblasts induce higher levels of functions in PHHs than liver sinusoidal endothelial cells[25], hepatic stellate cells[26], and Kupffer cells[27]. Importantly, the use of 3T3-J2 fibroblasts does not prevent the effective use of PHHs for many applications within the drug development pipeline[28–31] and significantly improves the sensitivity for the prediction of clinically relevant drug metabolism and toxicity than monocultures and randomly distributed cocultures[32]. However, it remains unclear whether 3T3-J2 fibroblasts can similarly sustain long-term functions in PMHs and enable a murine model for compound screening. Therefore, here we fabricated mouse MPCCs (mMPCCs) containing PMHs from different strains (C57Bl/6J and CD-1) and 3T3-J2 fibroblasts with empirically optimized dimensions. Cell morphology and major liver functions (albumin and urea secretion rates, and CYP1A, 2A, 2C, and 3A enzyme activities) in mMPCCs were assessed for 4 weeks. Last, we determined the utility of mMPCCs for in vivo relevant comparison studies across mouse strains and species (vs. MPCCs created using PHHs) for CYP induction and hepatotoxicity following exposure to 14 prototypical compounds.

MATERIALS AND METHODS

Isolation and Processing of Primary Mouse Hepatocytes (PMHs)

Animal use and husbandry followed protocols approved by the Hamner Institutes for Health Sciences Institutional Animal Care and Use Committee (Research Triangle Park, NC, USA) and were performed in accordance with the institutional guidelines. CD-1 and C57Bl6/J mice that were 6 weeks old were obtained from Charles River Laboratories (Durham, NC, USA). Animals were housed in groups of five in constant alternating 12-h light and dark cycles and allowed free access to food and water. PMHs were then isolated from these mice using a protocol approved by the Hamner Institutes for Health Sciences Institutional Animal Care and Use Committee. Briefly, the animals were anesthetized with isoflurane, and livers were perfused using a two-step collagenase method [6]. A catheter was inserted through the heart into the superior vena cava, and the liver was perfused first with divalent cation-free DMEM (Dulbecco's modified Eagle's medium)-based

buffer with EGTA [ethylene glycol-bis(-aminoethyl ether)-*N*,*N*,*N*′,*N*′-tetraacetic acid] at 37°C for 4 min, and then with Earle's balanced salt solution containing collagenase and protease (Vitacyte, Indianapolis, IN, USA) for 6–8 min. The liver was then excised and dissociated in Williams' E medium supplemented with 10% fetal bovine serum (FBS), 100 U/ml penicillin, 100 µg/ml streptomycin, 15 mM HEPES [4-(2-hydroxyethyl)-1-piperazineethanesulfonic acid], 0.1 µM dexamethasone, 4 µg/ml insulin, and 4 mM GlutaMAX™. Hepatocytes were filtered through a 105-µm nylon mesh, washed once by low-speed centrifugation, purified by Percoll® (GE Healthcare Life Sciences, Pittsburgh, PA, USA) gradient centrifugation, and transferred to a T-25 tissue culture flask placed on an orbital shaker (50 rpm) in an incubator (37°C, 5% CO_2) for 30 min. Cells were then washed by low-speed centrifugation and stored in cold storage medium (HypoThermosol®-FRS; BioLife Solutions, Bothell, WA, USA) for shipment.

Freshly isolated PMHs were shipped from the Hamner Institutes to Colorado State University (Fort Collins, CO, USA) or the University of Illinois at Chicago (Chicago, IL, USA). Following receipt of fresh hepatocytes, cells were centrifuged at 600 rpm for 8 min, and the supernatant was discarded and replaced with fresh medium. Cell viability was assessed using the trypan blue exclusion method and was found to be >90% for freshly isolated hepatocytes.

Establishment of Hepatocyte Cultures

Micropatterned cocultures (MPCCs) were created as previously described[33] and are illustrated in Figure 1. Briefly, adsorbed rat tail collagen I (Corning Life Sciences, Tewksbury, MA, USA) was lithographically patterned in each well of a 24-well plate to create 500-µm-diameter circular domains spaced 1,200 µm apart, center-to-center. PMHs selectively attached to the collagen domains leaving ~25,000 attached PMHs on ~90 collagen-coated islands within each well of a 24-well plate. Murine embryonic fibroblasts (3T3-J2) were seeded 18 to 24 h later at ~90,000 cells per well to create mMPCCs. Mouse micropatterned pure hepatocyte cultures (mMPHs), which did not receive murine fibroblasts, were used as density-matched controls. Hepatocyte culture medium containing a high-glucose DMEM (Corning Life Sciences) base was replaced on mMPCCs every 2 days (300 µl/well for a 24-well plate). Other components of the culture medium have been described previously[25].

For conventional monocultures, PMHs were diluted to a density of 1e6 cells/ml, seeded in collagen-coated plates (500 µl/well), and allowed to attach for 4 h. To complete an ECM protein mouse sandwich-cultured hepatocyte model (mSCH), Matrigel™ was added to the culture medium at 250 µg/ml, which caused a gelled overlay to form on the adherent PMHs. Culture medium was replaced after the first 24 h of seeding and every other day thereafter.

Morphological and Functional Assessments

Culture morphology was monitored under phase contrast using an EVOS®FL microscope (Thermo Fisher Scientific, Waltham, MA, USA). Culture supernatants were assayed for albumin levels using a competitive enzyme-linked immunosorbent assay (ELISA; MP Biomedicals, Santa Ana, CA, USA) with horseradish peroxidase detection and 3,3 ,5,5 -tetramethylbenzidine (TMB; Rockland Immunochemicals, Boyertown, PA, USA) as the substrate[23]. Urea concentration in culture supernatants was assayed using a colorimetric endpoint assay utilizing diacetyl monoxime with acid and heat (Stanbio Labs, Boerne, TX, USA)[23]. Absorbance values for the above

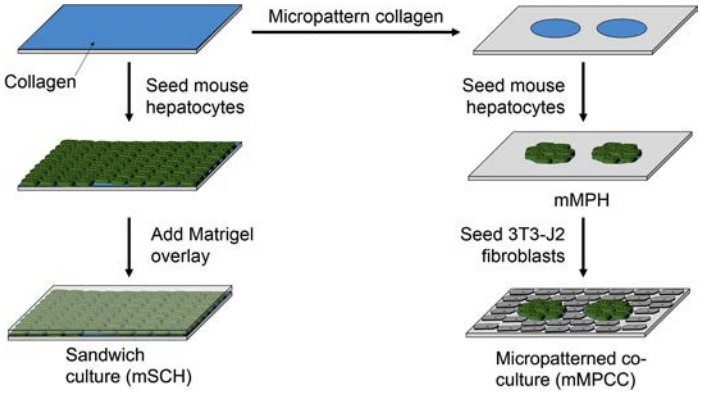

Figure 1. Fabrication of different mouse hepatocyte culture models. After tissue culture polystyrene was uniformly coated with rat tail collagen, three different culture models were established. Mouse sandwich-cultured hepatocytes (mSCH) adhered to the adsorbed collagen and were then sandwiched with a Matrigel™ overlay. Mouse micropatterned pure hepatocytes (mMPHs) were prepared using soft lithography techniques to micropattern the collagen into circular islands of a defined geometry and seeding mouse hepatocytes to fill the collagen islands. The mMPHs were surrounded by 3T3-J2 murine embryonic fibroblasts within 24 h to create mouse micropatterned cocultures (mMPCCs)[33].

assays were quantified using the Synergy H1 multimode plate reader (BioTek, Winooski, VT, USA).

CYP3A and CYP2C enzyme activities were measured by incubating the cultures with either luciferin-IPA (Promega Life Sciences, Madison, WI, USA) for 1 h or luciferin-H (Promega) for 3 h, respectively. The metabolite, luciferin, generated by CYP metabolism of the respective substrates was quantified via luminescence on the Synergy H1 multimode plate reader according to manufacturer's protocols. While luciferin-IPA has been used previously to determine the catalytic activity of CYP3A in mouse and human liver homogenates[34,35], luciferin-H has been validated only for CYP2C9 activity in human liver microsomes[35]; however, mouse CYP2C37 is highly homologous to CYP2C9[36].

CYP1A and CYP2A activities were measured by incubating the cultures with either 5 μM 7-ethoxyresorufin (Sigma-Aldrich, St. Louis, MO, USA) for 3 h or 50 μM coumarin (Sigma-Aldrich) for 1 h, respectively. The metabolites resorufin and 7-hydroxycoumarin (7-HC) generated via CYP1A- and CYP2A-mediated metabolism, respectively, of the abovementioned substrates were quantified via fluorescence on the Synergy H1 multimode plate reader [excitation/emission (nm): 550/585 for resorufin and 355/460 for 7-HC] using previously published protocols[33]. The activity of 7-ethoxyresorufin-O-deethylase is attributed to both mouse and human CYP1A[23,37]; coumarin 7-hydroxylase activity is also attributed to both mouse and human CYP2A[23,38].

Cell viability was quantified by the PrestoBlue™ assay (Thermo Fisher). Briefly, PrestoBlue substrate was combined with culture medium at a 1:9 ratio (v/v). The mixture was added to mMPCCs, incubated for 10 min, and the metabolite (resazurin) was quantified via fluorescence (560 nm excitation, 590 nm emission). ATP levels in cell lysates were determined using CellTiter-Glo™ (Promega). A 1:1 ratio (v/v) of CellTiter-Glo and culture medium was added to the cell layer, and luminescence from supernatants was quantified.

Drug Studies

For drug-mediated CYP induction studies, mMPCCs (7–10 days old) were exposed to serum-free culture medium containing rifampin (25 μM), phenobarbital (1 mM), -naphthoflavone (25 μM), dexamethasone (10 μM), omeprazole (50 μM), or dimethyl sulfoxide (DMSO) alone (0.1% v/v). Drugs were purchased from either Cayman Chemicals (Ann Arbor, MI, USA) or Sigma-Aldrich. CYP3A, CYP2C, and CYP1A enzyme activities were quantified after 4 days of drug exposure as described above. Data were normalized to a 0.1% (v/v) DMSO control to calculate fold changes.

For drug toxicity studies, mMPCCs (7–10 days old) were treated in serum-free medium to two concentrations of each drug (listed below), 25× and 100× C_{max} (C_{max} is the maximum human plasma concentration) every other day for a total of 6 days, a treatment timeframe previously found to provide an increase in sensitivity for drug toxicity detection without an increase in the false-positive rate over 1-day drug treatment in PHH/3T3-J2 cocultures[2]. Tolcapone, troglitazone, rosiglitazone, and ibufenac were purchased from Cayman Chemical, while nefazodone, buspirone, diclofenac, warfarin, and fialuridine were obtained from Sigma-Aldrich. All drugs were dissolved in 100% DMSO (Corning Life Sciences). The final DMSO concentration in the culture medium was kept at 0.1% (v/v) for all drugs except that 0.2% (v/v) was used for tolcapone, and 1.0% (v/v) was used for ibufenac due to limited solubility. The relevant DMSO controls at 0.1%, 0.2%, and 1% (v/v) were also maintained to calculate fold changes. Albumin and urea secretion rates, cell viability, and ATP levels were assessed as described above.

MPCCs containing cryopreserved PHHs (HUM4055A: 54-year-old female Caucasian and HUM4192: 16-year-old female Asian; purchased from Lonza, Walkersville, MD, USA) were created using the same protocol as mMPCCs. The PHH-MPCCs (7-10 days old) were then exposed to the same compounds for CYP induction or toxicity assessments as mMPCCs with the same dosing schedule and assays to evaluate functions and viability as detailed above.

Data Analysis

All findings were confirmed in independent experiments from at least two different donors of the same mouse strain. Data from a single representative donor/experiment is shown for each figure unless otherwise indicated. Data processing was performed using Microsoft Excel, and GraphPad Prism (La Jolla, CA, USA) was used for displaying results. For each assay, mean and standard deviation values were calculated using three technical replicates and normalized to the number of hepatocytes attached in each well. For the drug exposure studies, functions in all treated cultures were compared to functions in DMSO-only controls, and functional data are reported as percentages of that control. IC_{50} values (drug concentrations that reduced an endpoint signal by at least 50% of DMSO-only controls) were calculated by the linear interpolation between the drug dose at which the assay signal was $>50\%$ of controls and the drug dose at which the assay signal was $<50\%$ of controls. Statistical significance was determined with a one- or two-way ANOVA followed by a Bonferroni pairwise post hoc test ($p<0.05$).

RESULTS

Characterization of PMH Monocultures

Upon seeding into collagen-coated wells and overlaying with Matrigel™, C57Bl/6J PMHs in such an mSCH

culture format (Fig. 1) showed prototypical hepatic morphology with a polygonal shape, multinucleation, and distinct nuclei/nucleoli (Fig. 2A). However, PMHs lost their cuboidal morphology and became spread and flattened in mSCHs over 1–2 weeks of culture (Fig. 2B and C). Similar morphological trends were observed with C57Bl/6J PMHs seeded into a micropatterned format without supportive fibroblasts or mMPHs (Fig. 2D–F). At a functional level, mSCH cultures displayed a rapid decline in albumin (i.e., day 7 levels dropped to 23% of day 3 levels) and urea (i.e., day 7 levels dropped to 29% of day 3 levels) secretion rates (Fig. 2G). CYP3A activity also declined in mSCH cultures; day 7 levels dropped to 16% of day 3 levels (Fig. 2H). In contrast, mMPHs had significantly higher albumin/urea secretion rates (Fig. 2G) and CYP3A activity (Fig. 2H) than mSCH cultures. Specifically, albumin and urea secretion rates, and CYP3A activity in mMPHs were 1.8-fold, 12-fold, and 8-fold higher than mSCH on day 3, respectively. However, by day 7, these functions had declined to negligible levels in both types of monoculture models.

Characterization of C57Bl/6J mMPCCs With a Comparison to ECM Sandwich Cultures

Rat tail collagen I was micropatterned into circular domains within 24-well plates using a soft lithographic process utilizing a polydimethylsiloxane (PDMS) mask[33]. PMHs selectively attached to the micropatterned collagen domains and were surrounded the next day with 3T3-J2 murine embryonic fibroblasts (Fig. 1). Circular collagen domains of 500-μm diameter with 1,200-μm center-to-center spacing have been shown previously to stabilize the functions of primary rat[14] and human hepatocytes[23] in coculture with 3T3-J2 fibroblasts. Here the collagen island diameter and spacing were varied for mMPCCs toward determining the effects on the levels of hepatic functions (Fig. 3A). Higher hepatic functions were observed when less surface area in each well was occupied by PMHs, and the remaining surface area

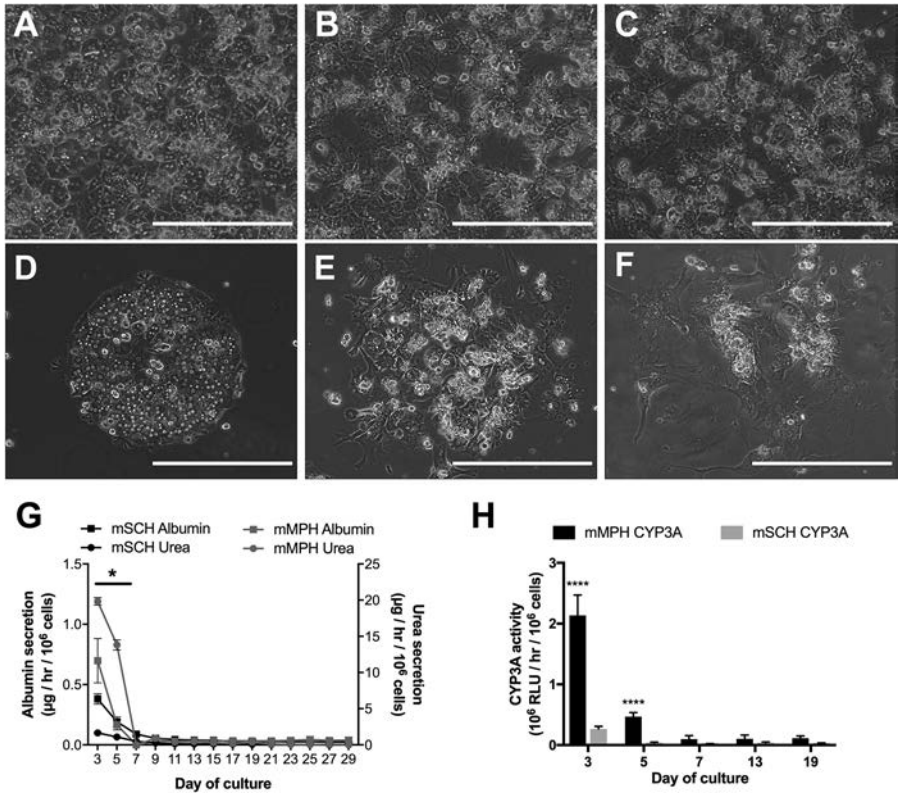

Figure 2. Morphology and liver functions of C57Bl/6J primary mouse hepatocytes in monoculture formats. Freshly isolated C57Bl/6J mouse hepatocytes were adhered to adsorbed collagen and then sandwiched with a Matrigel™ overlay (mSCHs). Prototypical cuboidal hepatocyte morphology in mSCHs after (A) 1 day of seeding degraded after (B) 1 week and (C) 2 weeks of culture. Similarly, mMPHs devoid of fibroblasts showed normal morphology of mouse hepatocytes after (D) 1 day of culture that degraded after (E) 1 week and (F) 2 weeks of culture. Scale bars: 400 μm. At the functional level, both mSCHs and mMPHs showed a rapid decline of (G) albumin and urea secretion rates and (H) CYP enzyme activities. Error bars represent standard deviations ($n = 3$). *$p < 0.05$, ****$p < 0.0001$ between the mSCH and mMPH conditions.

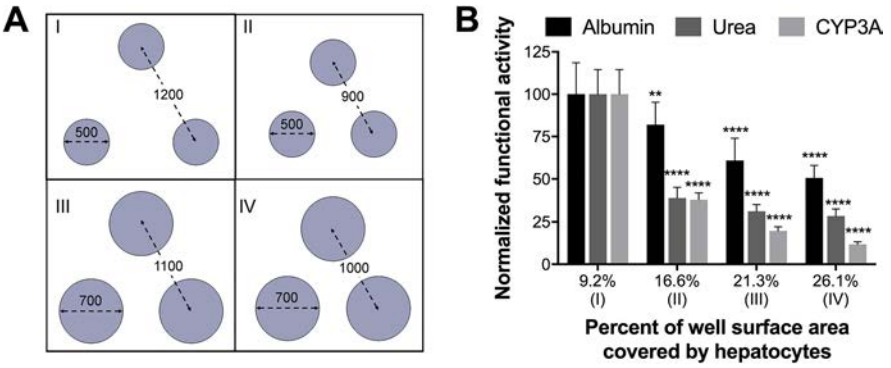

Figure 3. Dependency of micropatterned coculture functions on collagen island architecture (diameter and spacing). (A) Various micropatterned geometries (i.e., confluent clusters) allowed mouse hepatocytes to cover 9.2% (500-µm island diameter with 1,200-µm center-to-center spacing), 16.6% (500-µm diameter, 900-µm center-to-center), 21.3% (700-µm diameter, 1,100-µm center-to-center), or 26.1% (700-µm diameter, 1,000-µm center-to-center) of the available surface area in each well of an industry standard 24-well plate. All dimensions shown are in microns. (B) Albumin and urea secretion rates, and CYP3A activity from a representative time point (day 15) are shown, although similar trends were observed over multiple weeks. All data were normalized to the 9.2% geometry (500-µm diameter, 1,200-µm center-to-center). Error bars represent standard deviations ($n = 3$). $^{**}p < 0.01$, $^{****}p < 0.0001$ between the 9.2% geometry and the other geometries.

was available for fibroblast attachment (Fig. 3B); thus, the optimal architecture for mMPCCs was also found to be circular collagen domains of 500-µm diameter with 1,200-µm center-to-center spacing.

C57Bl/6J PMHs showed prototypical hepatic morphology on the day of seeding onto micropatterned collagen domains (Fig. 4A). PMHs were retained on the islands with the surrounding fibroblasts in C57Bl/6J mMPCCs for at least 4 weeks (Fig. 4B and C). At the functional level, mMPCCs secreted albumin and urea for 4 weeks (Fig. 4D), at significantly higher rates than the density-matched mMPHs (e.g., ~12-fold higher for albumin and ~2.6-fold higher for urea on day 11 of culture). Similarly, the activities of CYP3A (Fig. 4E), CYP1A (Fig. 4F), and CYP2C (Fig. 4G) were higher in mMPCCs over the course of 4 weeks than mMPHs. For instance, CYP3A, CYP1A, and CYP2C activities in mMPCCs after 23 days were ~2-fold, 6.4-fold, and 3-fold higher than those in mMPHs, respectively. However, CYP2A activity in C57Bl/J6 mMPCCs was negligible compared to activity in PHH-MPCCs (Fig. 5). The 3T3-J2 fibroblasts were found to be devoid of any of the measured liver functions, including albumin secretion, urea synthesis, and CYP activities (data not shown). Last, while no bile canaliculi were visible in mMPHs after 3 weeks of culture, PMHs in mMPCCs formed functional bile canaliculi, as assessed by the active transporter-mediated excretion of fluorescent 5 (and 6)-carboxy-2 ,7 -dichlorofluorescein (CDF) into the bile canaliculi between adjacent hepatocytes (Fig. 6A).

Compared to collagen/Matrigel™ mSCHs created from C57Bl/6J PMHs, urea secretion rate in C57Bl/6J mMPCCs was ~62-fold, 413-fold, and 548-fold higher after 5, 11, and 19 days, respectively (Fig. 2G vs. Fig. 4D). Albumin secretion rates were ~6.5-fold, 143-fold, and 305-fold higher in mMPCCs than in mSCHs after 5, 11, and 19 days, respectively (Fig. 2G vs. Fig. 4D). Finally, CYP3A activities were 14-fold and 10-fold higher in mMPCCs than in mSCHs after 5 and 17 days (19 days for mSCH), respectively (Fig. 2H vs. Fig. 4E).

To determine if the 3T3-J2 murine embryonic fibroblasts could be replaced with human fibroblasts, we created C57Bl/6J mMPCCs with either adult or neonatal human dermal fibroblasts. However, neither of the human fibroblasts was able to maintain prototypical morphology and functions (albumin and urea secretion rates) of PMHs to the same extent as the 3T3-J2 fibroblasts (Fig. 7). Similar trends were also observed with PHHs and dermal fibroblasts in MPCCs (data not shown), thereby suggesting the beneficial effects of 3T3-J2 fibroblasts on hepatocytes from both mouse and human species.

Characterization of CD-1 mMPCCs

As with C57Bl/6J PMHs, CD-1 PMHs showed prototypical hepatic morphology (polygonal shape, distinct nuclei/nucleoli) on the day of seeding onto micropatterned collagen domains (Fig. 8A). CD-1 PMHs were retained on the islands with the surrounding fibroblasts in mMPCCs for at least 4 weeks (Fig. 8B and C). At the functional level, CD-1 mMPCCs secreted albumin and urea for 4 weeks (Fig. 8D), at significantly higher rates than mMPHs (e.g., ~19-fold higher for albumin and ~5-fold higher for urea on day 11 of culture). Similarly, the activities of CYP3A (Fig. 8E), CYP1A (Fig. 8F), and CYP2C (Fig. 8G) were higher in CD-1 mMPCCs over 4 weeks than mMPHs. For instance, CYP3A, CYP1A, and CYP2C activities in CD-1 mMPCCs after 23 days were

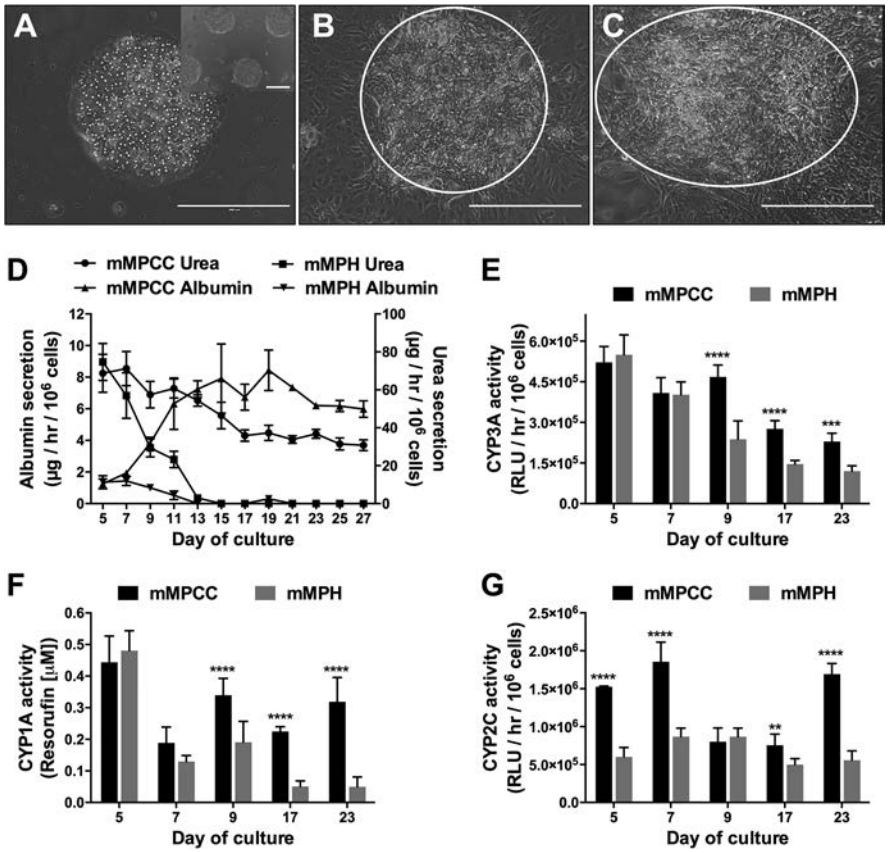

Figure 4. Morphology and liver functions of C57Bl/6J primary mouse hepatocytes in micropatterned culture formats. (A) Freshly isolated C57Bl/6J mouse hepatocytes can be micropatterned onto collagen-coated circular domains (mMPHs) and display prototypical morphology under phase contrast on the day of seeding and prior to coculture with 3T3-J2 fibroblasts. In mMPCCs containing the fibroblasts, hepatocytes retain their morphological features after (B) 1 week and (C) 2 weeks in culture. All scale bars represent 400 µm. (D) Time series of albumin and urea secretion rates in C57Bl/6J mMPCCs and mMPHs. (E–G) Time series of CYP3A, CYP1A, and CYP2C enzyme activities in mMPCCs and mMPHs. Error bars represent standard deviations ($n = 3$). $^{**}p < 0.01$, $^{***}p < 0.001$, $^{****}p < 0.0001$ between the mMPCC and mMPH conditions.

~9-fold, 21.7-fold, and 9.2-fold higher than mMPHs, respectively. However, CYP2A activity in CD-1 mMPCCs was negligible compared to activity in PHH-MPCCs (Fig. 5). Last, while no bile canaliculi were visible in mMPHs after 3 weeks, CD-1 PMHs in mMPCCs formed functional bile canaliculi (Fig. 6B).

When comparing functions in C57Bl/6J and CD-1 mMPCCs, similarities and differences were observed. Specifically, albumin and urea secretion kinetics, as well as urea levels, were similar across the two strains, while CD-1 mMPCCs displayed approximately two-fold higher albumin secretion rate than C57Bl/6J mMPCCs (Fig. 4D vs. Fig. 8D). CYP3A activity in C57Bl/6J mMPCCs was ~1.7-fold higher than activity measured in CD-1 mMPCCs (Fig. 4E vs. Fig. 8E); CYP1A activities across the two strains were similar (Fig. 4F vs. Fig. 8F); and CYP2C9 activity in C57Bl/6J mMPCCs was ~3- to 5-fold higher than activity measured in CD-1 mMPCCs (Fig. 4G vs. Fig. 8G).

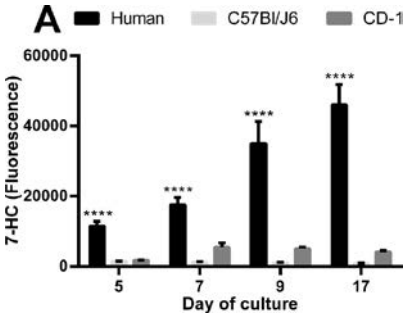

Figure 5. CYP2A enzyme activity in MPCCs created using C57Bl/6J or CD-1 primary mouse hepatocytes or primary human hepatocytes. Freshly isolated C57Bl/6J and CD-1 primary mouse hepatocytes or cryopreserved primary human hepatocytes were incorporated into MPCCs. CYP2A activity at the indicated time points was assessed using coumarin conversion to fluorescent 7-hydroxycoumarin (7-HC). Error bars represent standard deviations ($n = 3$). $^{****}p < 0.0001$ between human MPCCs and both mouse strains.

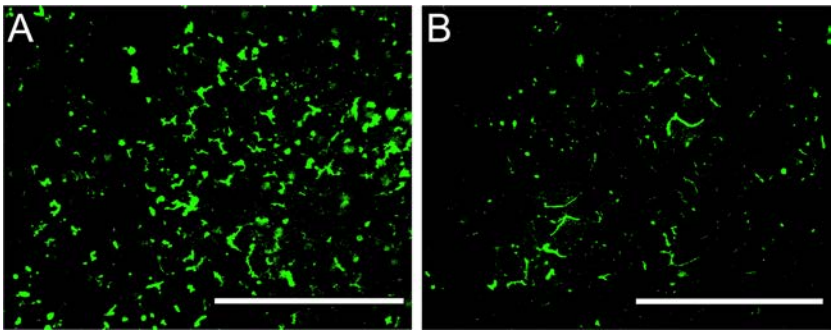

Figure 6. Functional bile canaliculi in mMPCCs. After 3 weeks in culture, mMPCCs containing either (A) C57Bl/6J or (B) CD-1 primary mouse hepatocytes were incubated with fluorescent CDF [5-(and 6)-carboxy-2 ,7 -dichlorofluorescein diacetate], which is taken up by hepatocytes and excreted into the bile canaliculi between adjacent hepatocytes. Scale bars: 400 µm.

Drug-Mediated CYP Induction in mMPCCs Versus PHH-MPCCs

C57Bl/6J or CD-1 mMPCCs were treated with prototypical enzyme inducers (rifampin at 25 µM, phenobarbital at 1 mM, dexamethasone at 10 µM, omeprazole at 50 µM, and -naphthoflavone at 25 µM) for 4 days followed by assessment of CYP3A, CYP2C, and CYP1A enzyme activities using luciferin-IPA, luciferin-H, and 7-ethoxyresorufin substrates, respectively. Across both strains, CYP3A was induced by rifampin (~14- to 17-fold relative to DMSO-treated controls), phenobarbital (~8- to 10-fold), and dexamethasone (~23- to 31-fold); CYP1A was induced by -naphthoflavone (~4- to 8-fold), and CYP2C was induced by rifampin (~1.6- to 1.8-fold) (Fig. 9). Omeprazole, however, did not

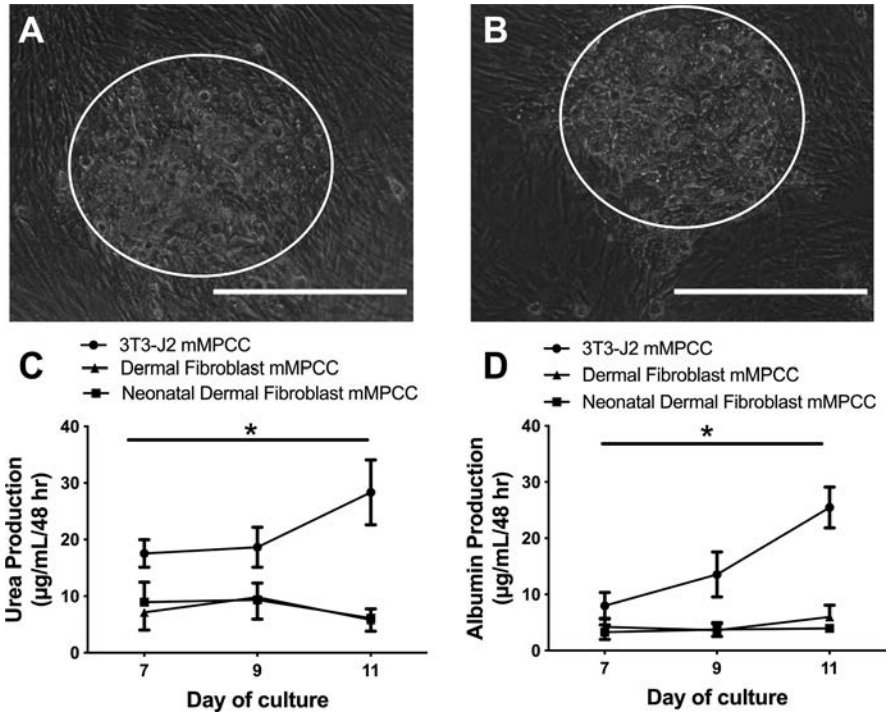

Figure 7. Morphology and functions in mMPCCs containing primary mouse hepatocytes and different types of fibroblasts. Phase-contrast pictures of C57Bl/6J primary mouse hepatocytes cocultured with either (A) adult human dermal fibroblasts or (B) neonatal human dermal fibroblasts (human fibroblasts were obtained from American Type Culture Collection, Manassas, VA, USA and cultured according to manufacturer's protocols). Scale bars: 400 µm. Time series of (C) urea and albumin secretion rates in different mMPCCs, including those created using 3T3-J2 murine embryonic fibroblasts. $*p < 0.05$ between 3T3-J2 mMPCCs and the other two mMPCC models.

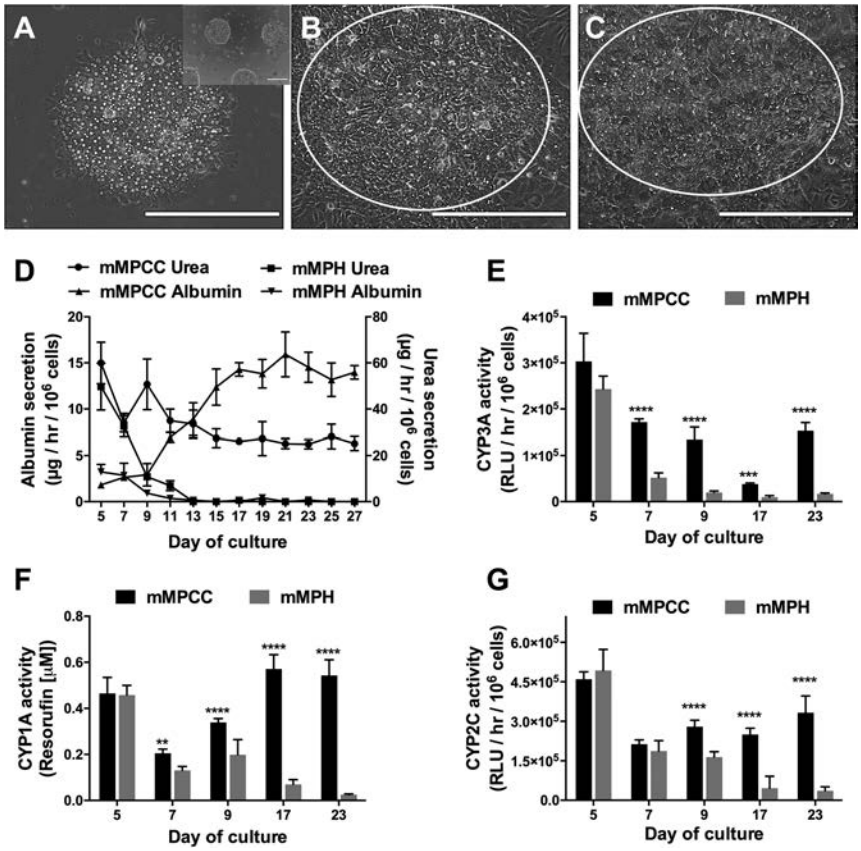

Figure 8. Morphology and liver functions of CD-1 primary mouse hepatocytes in micropatterned culture formats. (A) Freshly isolated CD-1 mouse hepatocytes can be micropatterned onto collagen-coated circular domains (mMPHs) and display prototypical morphology under phase contrast on the day of seeding and prior to coculture with 3T3-J2 fibroblasts. In mMPCCs containing the fibroblasts, hepatocytes retain their morphological features after (B) 1 week and (C) 2 weeks in culture. All scale bars represent 400 µm. (D) Time series of albumin and urea secretion rates in CD-1 mMPCCs and mMPHs. (E–G) Time series of CYP3A, CYP1A, and CYP2C enzyme activities in mMPCCs and mMPHs. Error bars represent standard deviations ($n = 3$). $^{**}p < 0.01$, $^{***}p < 0.001$, $^{****}p < 0.0001$ between mMPCC and mMPH conditions.

cause statistically significant induction of any of the tested CYP isozymes across both mouse strains, whereas it was a potent inducer of CYP1A in PHH-MPCCs (Fig. 10).

Drug Toxicity in mMPCCs Versus PHH-MPCCs

C57Bl/6J or CD-1 mMPCCs were treated with six human hepatotoxic drugs and three nonhepatotoxic drugs (Table 1) over 6 days, with fresh drug added to culture medium with every 2-day medium exchange; drug concentrations chosen were 25× and 100× C_{max} (C_{max} is the maximum human plasma concentration). At the end of the drug treatment, PMH functions (albumin and urea secretion rates) and overall mMPCC viability (ATP in cell lysates and PrestoBlue™ conversion to resazurin) were assessed. For comparison, PHH-MPCCs were also treated for 6 days to the nine drugs and assessed for functions and viability as described above. IC_{50} values for each endpoint were calculated as multiples of each drug's C_{max}.

For diclofenac, nefazodone, and tolcapone, both CD-1 and C57Bl/6J mMPCCs displayed toxicity across all endpoints at the tested drug concentrations with statistically similar IC_{50} values across the two mouse strains (Table 1). For troglitazone, C57Bl/6J mMPCCs, but not CD-1 mMPCCs, displayed toxicity across all endpoints. For ibufenac and fialuridine, neither C57Bl/6J mMPCCs nor CD-1 mMPCCs displayed toxicity across any of the endpoints at the tested drug concentrations. On the other hand, PHH-MPCCs accurately displayed toxicity to all tested toxins; when toxicity was observed in either or both mouse strains in mMPCCs, IC_{50} values were statistically similar to responses in PHH-MPCCs. Last, none of the nonhepatotoxic drugs (buspirone, rosiglitazone, and warfarin) displayed toxicity in mMPCCs from both strains and PHH-MPCCs.

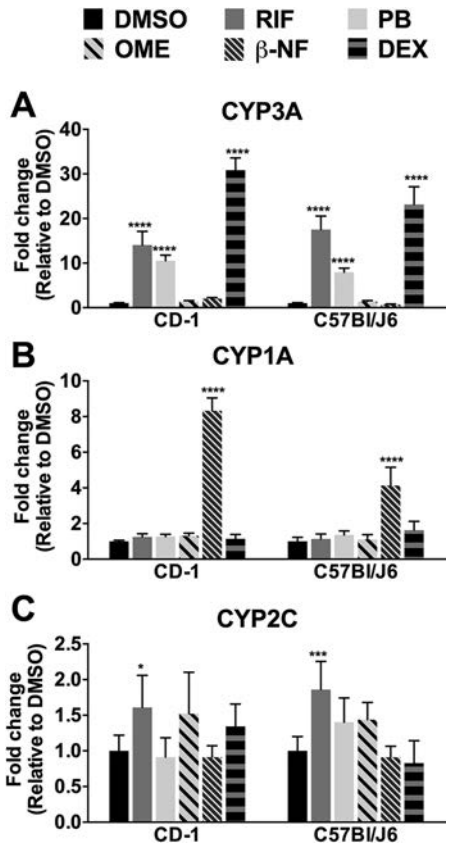

Figure 9. Drug-mediated induction of CYP enzyme activities in C57Bl/6J and CD-1 mMPCCs. Freshly isolated C57Bl/6J and CD-1 mouse hepatocytes were incorporated into the mMPCC platform, allowed to functionally stabilize for ~1 week, and treated with 0.1% (v/v) DMSO, 25 μM rifampin (RIF), 1 mM phenobarbital (PB), 50 μM omeprazole (OME), 25 μM -naphthoflavone (-NF), or 10 μM dexamethasone (DEX) for 4 days. (A) CYP3A, (B) CYP1A, and (C) CYP2C enzyme activities were then quantified using the appropriate luminescent or florescent assay (see Materials and Methods). Data are plotted as fold change with respect to the DMSO control (fold change = 1). Error bars represent standard deviations ($n = 3$). *$p < 0.05$, ***$p < 0.001$, ****$p < 0.0001$ between the drug-treated condition and DMSO control.

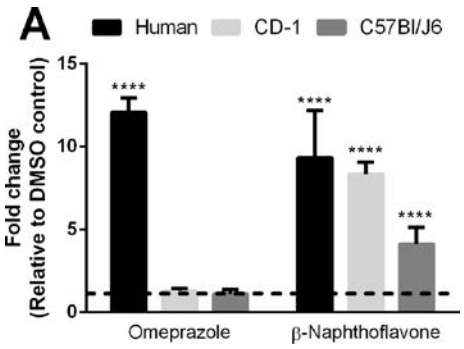

Figure 10. Drug-mediated CYP1A induction in MPCCs created using C57Bl/6J or CD-1 primary mouse hepatocytes or cryopreserved primary human hepatocytes. Freshly isolated C57Bl/6J and CD-1 primary mouse hepatocytes or cryopreserved primary human hepatocytes were incorporated into MPCCs, allowed to functionally stabilize for ~1 week, and treated with 0.1% (v/v) DMSO, 25 μM -naphthoflavone, or 50 μM omeprazole for 4 days. CYP1A enzyme activity was quantified using ethoxyresorufin conversion to fluorescent resorufin. Data are plotted as fold change with respect to DMSO control (dashed line). Error bars represent standard deviations ($n = 3$). ****$p < 0.0001$ between drug-treated condition and DMSO control.

DISCUSSION

Genetically diverse mouse strains are a promising tool for characterizing compound effects across different subpopulations and identifying genetic determinants underlying susceptibility to severe drug toxicity in humans. Since hepatotoxicity is a leading cause of compound attrition, in vitro liver platforms help prioritize compounds for in vivo testing; however, PMH functions decline rapidly in monocultures. In contrast, we show here for the first time that PMHs maintain liver functions, including drug metabolism capacities, for 4 weeks in mMPCCs containing 3T3-J2 fibroblasts, which subsequently enabled in vivo relevant comparisons across strains and species (vs. PHH-MPCCs) for drug-mediated CYP induction and hepatotoxicity.

We created collagen/Matrigel ECM sandwich cultures of C57Bl/6J PMHs and observed a rapid and expected phenotypic decline within days. In contrast, when PMHs were arranged onto micropatterned collagen islands, such that confluent clusters of PMHs were obtained while using ~9–10% of the well's surface area for PMH attachment, liver functions improved up to 12-fold relative to sandwich cultures. Nonetheless, functions in both types of monocultures declined to negligible levels after 7 days, suggesting that micropatterning alone is not sufficient to stabilize PMH functions.

Since 3T3-J2 murine embryonic fibroblasts have been previously shown to stabilize the functions of primary rat[14] and primary human hepatocytes[23] for several weeks in vitro, here we combined the functional benefits of micropatterning with 3T3-J2 fibroblasts to create mouse micropatterned cocultures (mMPCCs). Circles were chosen for the shape of the micropatterned collagen because, in contrast to patterns with sharp corners, circles allow better retention of patterning fidelity and thus homotypic interactions over several weeks in our experience[32]. The diameter and spacing of the circular collagen islands were further optimized to enable high mMPCC functions; the optimal architecture was found to be 500-μm-diameter islands with 1,200-μm center-to-center spacing, previously also found to be optimal for PHHs in MPCCs[23] but not MPCCs containing primary rat hepatocytes[14].

Interestingly, all tested hepatic functions (albumin, urea, and CYP3A) showed an inverse relationship with

Table 1. IC_{50} Values for Compounds Tested in Primary Mouse and Human Hepatocytes in Micropatterned Cocultures (MPCCs)

		Albumin			Urea			Cell Viability			ATP		
Compound	C_{max} (μM)	CD-1	C57	Human	CD-1	C57	Human	CD-1	C57	Human	CD-1	C57	Human
Diclofenac	8.023	43.6 ± 28.4	56.1 ± 6.8	57.0 ± 7.6	53.2 ± 2.0	48.7 ± 12.4	44.0 ± 26.2	71.6 ± 8.6	73.0 ± 0.7	37.6 ± 32.2	59.8 ± 3.0	63.9 ± 1.9	37.1 ± 34.8
Fialuridine	1.000	–	–	40.7 ± 30.8	–	–	13.6 ± 1.4	–	–	80.4 ± 0.1	–	–	79.7 ± 7.8
Ibufenac	0.100	–	–	66.8 ± 23.3	–	–	54.7 ± 4.5	–	–	75.4 ± 30.8	–	–	70.4 ± 41.9
Nefazodone	0.001	76.5 ± 3.6	58.8 ± 9.1	37.6 ± 35.2	77.9 ± 31.3	76.7 ± 10.0	28.4 ± 22.2	73.3 ± 1.5	73.6 ± 1.1	38.2 ± 35.7	80.3 ± 27.9	60.3 ± 0.6	37.6 ± 35.5
Tolcapone	0.018	62.6 ± 14.8	37.8 ± 32.1	18.6 ± 8.6	56.3 ± 9.0	37.3 ± 32.6	28.4 ± 22.5	55.8 ± 14.5	49.1 ± 37.9	31.0 ± 24.9	62.5 ± 0.1	37.7 ± 33.2	36.2 ± 33.3
Troglitazone	6.387	–	63.6 ± 4.5	77.8 ± 31.4	–	80.5 ± 27.7*	42.73 ± 28.0	–	85.8 ± 20.1	77.89 ± 18.8	–	67.2 ± 15.4	60.7 ± 52.9
Buspirone	0.005	–	–	–	–	–	–	–	–	–	–	–	–
Rosiglitazone	1.120	–	–	–	–	–	–	–	–	–	–	–	–
Warfarin	4.868	–	–	–	–	–	–	–	–	–	–	–	–

Values listed are IC_{50} values (average ± standard deviation from $n = 2$ donors), the interpolated drug concentration that reduces a biochemical signal by 50%, presented as multiples of C_{max} (maximum concentration observed in human plasma). "–" represents an IC_{50} value above $100 \times C_{max}$ (i.e., could not be interpolated from the dose range tested here) and declared to be "nonhepatotoxic" by our algorithm. C57 refers to the C57Bl/6J mouse strain. Italicized drug names represent nonhepatotoxic drugs, while the nonitalicized drugs are typically considered hepatotoxins in humans. There are no statistically significant differences in interpolated IC_{50} values comparing human to mouse and across mouse strains based on a one-way ANOVA analysis.

percent of surface area in each well that was occupied by the PMHs, and the remaining surface area was available for fibroblast attachment. Specifically, of the four surface areas tested (9.2%, 16.6%, 21.3%, 26.1%) via modulation of circular collagen domain diameters and/or spacing, the 9.2% surface area, which corresponds to the optimal architecture above (diameter/center-to-center spacing: 500 μm/1,200 μm), had the highest functional output. We did not test surface areas less than 9.2% because the sensitivity of some of the endpoint assays (e.g., detection of drug metabolites) can be compromised with much fewer PMHs in each well. While the exact molecular mechanism underlying this inverse relationship between surface area covered by PMHs and functional output is not known and would necessitate follow-up investigations, we speculate that the optimal architecture yields high hepatic functions due to a) a restriction in the number of PMHs within each well given their high oxygen consumption rate that exceeds even that of rat and human hepatocytes[12], b) collagen micropatterning that allows clustering of the PMHs and the formation of the cadherin and tight junctions, which are essential for hepatic functions and polarity as also observed in hepatocytes from rats[14] and humans[23], c) an optimal ratio between PMHs and the 3T3-J2 fibroblasts (1:3), and d) stimulation by liver-like molecules presented by the 3T3-J2 fibroblasts, such as decorin[21] and T-cadherin[22], albeit the complete list of molecules involved in the interactions between the 3T3-J2 fibroblasts and PMHs has yet to be elucidated. Nonetheless, as we have shown here, the use of this fibroblast clone does not prevent the effective use of PMHs for CYP induction and drug toxicity assays.

PMHs from C57Bl/6J (inbred) and CD-1 (outbred) mice were retained for several weeks in mMPCCs. However, bile canaliculi in mMPCCs were not as extensive as those in rat[39] and human[23] hepatocytes in MPCCs, which may be due to a higher level of integration of the mouse fibroblasts within the PMH colonies. Regardless, liver functions were retained for 4 weeks in mMPCCs at higher levels than sandwich cultures (e.g., 300- to 500-fold higher after 3 weeks). Urea and CYP1A activity were similar across the two strains, whereas albumin, CYP3A, and CYP2C varied across the strains between 1.7- and 5-fold. Further studies in live mice from these strains under identical nutritional conditions are needed to appraise the degree of correlation between in vitro and in vivo functions. Nevertheless, PMHs from both strains showed high levels of functions in mMPCCs over a similar timeframe, suggesting that the culture technique is useful for multiple strains. In contrast to CYP1A, CYP3A, and CYP2C, the activity of CYP2A, as assessed by coumarin 7-hydroxylation, was negligible in mMPCCs, but high in PHH-MPCCs, which is a species-specific difference also previously observed in liver microsomes[40]. Last, the

use of human dermal fibroblasts (adult or neonatal) in mMPCCs did not increase bile canaliculi due to the species mismatch (as in PHH-MPCCs) to restrict the integration of mouse fibroblasts within the mouse hepatocyte colonies; the dermal fibroblasts also could not induce either PMH (or PHH) functions to the same levels as the 3T3-J2 fibroblasts. Therefore, the 3T3-J2 fibroblasts can help maintain liver-specific function for at least 4 weeks in primary hepatocytes from both mouse and human.

Many compounds induce CYP enzymes by activating nuclear receptors, which can affect the efficacy and/or toxicity of coadministered compounds[41]. Thus, we incubated mMPCCs with five prototypical CYP inducers for 4 days and assessed CYP activities. Both strains responded to inducer drugs similarly. CYP3A was induced by rifampin, phenobarbital, and dexamethasone, likely due to the activation of pregnane X receptor (PXR) by rifampin and dexamethasone[42], and activation of constitutive androstane receptor (CAR) by phenobarbital[43]. CYP2C was induced by rifampin, and CYP1A was induced by -naphthoflavone, an activator of the aryl hydrocarbon receptor (AhR)[44]. When comparing CYP induction in mMPCCs and PHH-MPCCs, similarities and differences were noted. Rifampin, phenobarbital, and dexamethasone induced CYP3A, rifampin induced CYP2C, and -naphthoflavone induced CYP1A across both species within similar fold change ranges when accounting for donor-dependent differences[23,33]. On the other hand, omeprazole (AhR activator) induced CYP1A in PHH-MPCCs but not mMPCCs, a finding consistent with previous findings in PMH monocultures and in vivo mouse studies[45,46]. Therefore, mMPCCs provide a useful model to determine human-relevant compound-mediated CYP induction for several compounds, while allowing for appraisal and further investigation of any species-specific differences for certain compound classes.

Next, we treated mMPCCs and PHH-MPCCs with six human hepatotoxic and three nonhepatotoxic drugs for 6 days, which can improve the sensitivity for drug toxicity detection in in vitro hepatocyte cultures without increasing the false-positive rate relative to 1-day treatment[2]. For each compound, we tested 25× and 100× C_{max}; the use of drug concentrations up to 100× C_{max} accounts for variable drug concentrations observed in human blood and within the liver due to potential polymorphisms in hepatic drug metabolism/transporter pathways but does not increase the false-positive rate of liver toxicity assays[2,47,48]. Additionally, we evaluated albumin and urea secretion rates as markers of PMH functions, and metabolism of resazurin-based PrestoBlue™ and ATP in cell lysates as markers of coculture viability; downregulation of albumin/urea secretion rates has been shown to correlate with compound-induced hepatotoxicity[2,47,49,50]. A compound was considered "toxic" only if IC_{50} values could be interpolated with the concentration range tested for at least one coculture viability marker and one hepatocyte functional marker.

Both mMPCCs and PHH-MPCCs experienced toxicity to diclofenac, nefazodone, and tolcapone, with statistically similar IC_{50} values across the two tested mouse strains (C57Bl/6J and CD-1) and when comparing compound effects in mouse and human using two donors. Determination of a larger range of donor variations in dose-dependent compound effects across mouse and human hepatocytes will necessitate a larger set of compound concentrations and >10 donors for PMHs and PHHs; nonetheless, our proof-of-concept study shows that mMPCCs are suitable to evaluate the species-relevant toxicity of the three compounds above. Finally, C57Bl/6J mMPCCs and PHH-MPCCs, but not CD-1 mMPCCs, experienced toxicity to troglitazone. In vivo studies with CD-1 mice have shown that while there are microscopic changes in the liver upon troglitazone administration for 3 weeks, no other toxicologically significant changes were observed[51]; in contrast, troglitazone toxicity has been detected in vivo in C57Bl/6J mice susceptible to increased mitochondrial stresses[52,53].

Fialuridine and ibufenac were toxic to PHH-MPCCs but not mMPCCs. It is known that fialuridine, a nucleoside analog drug for hepatitis B viral infection that caused liver failure and the deaths of five patients in clinical trials due to lactic acidosis, does not cause toxicity to mice, likely due to differential incorporation into mitochondrial DNA across different species[54,55]. For ibufenac, a nonsteroidal anti-inflammatory drug withdrawn from the market due to hepatotoxicity, further investigation of metabolism and transport in PMHs and PHHs is necessary in the future to determine the mechanisms underlying the species differences.

Overall, CD-1 and C57Bl/6J mMPCCs detected the toxicity of three and four human hepatotoxic drugs, respectively, whereas PHH-MPCCs detected the toxicity of all six drugs. These results suggest that C57Bl/6J PMHs are more sensitive for the detection of human-relevant compound-induced hepatotoxicity; however, testing in CD-1 PMHs may allow determination of why specific humans are resistant to the severe toxicity of certain compounds. Furthermore, neither mMPCCs nor PHH-MPCCs experienced toxicity to the three nonhepatotoxins, suggesting a high specificity (low false-positive rate) across the culture models at the compound concentration range tested (up to 100× C_{max}). Ultimately, testing compounds in PMHs from a larger cohort of genetically diverse mice (e.g., the Collaborative Cross) can shed insights into the genetic determinants underlying variable compound toxicity in humans.

The MPCC platform offers key advantages over other available liver culture formats for applications in compound development (Table 2). First, MPCCs provide the opportunity for higher-throughput compound testing in

multiwell plates than microfluidic cultures that require complex perfusion equipment, which restricts testing to a few devices (<12) in any given experiment. Here we created mMPCCs in 24-well plates for medium-throughput studies, though adaption to 96- and 384-well plate formats is likely possible with the optimization of seeding and culturing parameters as previously done for PHH-MPCCs[2,56]. Second, the function of hepatocytes in MPCCs is maintained over several weeks even while using much fewer cells (~10%) than bioprinted livers and randomly distributed (conventional) cultures/cocultures; thus, many compounds can be screened on demand and longitudinally in MPCCs that are created with the same batch of cryopreserved hepatocytes. Third, the MPCC approach has now been shown to sustain long-term (3+ weeks) functions of primary human[23], rat[14], dog[57], monkey[58], and now with this body of work, mouse hepatocytes; the use of a similar culture technique and supportive 3T3-J2 fibroblasts allows investigators to compare species-specific drug effects as we have shown here when comparing drug-mediated CYP induction and drug toxicity in mouse versus human MPCCs.

The long-lasting mMPCCs developed here can serve as a base platform for future improvements to model

Table 2. Benefits and Limitations of Current Liver Culture Platforms

Model	Benefits	Potential Limitations
Randomly distributed cultures and cocultures[6,58,59]	No specialized equipment needed to culture in standard multiwell plates ECM sandwich maintains cell polarity for a few days Useful for short-term drug assays	Significant loss of drug metabolism enzyme activity within hours to a few days in sandwich cultures, including in mouse hepatocytes as shown here
Micropatterned cocultures[22,23,60]	Control over homotypic and heterotypic cell–cell interactions enable 3+ weeks of functions in hepatocytes from multiple species, including mouse as shown here Compatible with standard multiwell plates Allow inclusion of liver nonparenchymal cells Useful for short- and long-term drug assays	Require specialized equipment and devices for patterning ECM proteins for hepatocyte attachment Single configuration containing all major liver cell types is currently lacking Use nonliver fibroblasts for inducing optimal functions in hepatocytes
Static self-assembled spheroids[13,60,61]	Can be created using off-the-shelf ultra-low attachment plates Enable cell–cell interactions in three dimensions Maintain liver functions for several weeks Useful for short- and long-term drug assays	Difficult to control multicellular interactions given heterogeneous architecture Necrosis in the center of larger (> 300 μm) spheroids Incompatible with standard microscopy techniques (requires confocal imaging) Not clear if mouse hepatocyte functions can be sustained beyond a few days
Bioprinted livers[62]	Precise control of cell placement allows the formation of separate cell type compartments in a single tissue Diverse architectures can be created as desired Maintain liver functions for several weeks Useful for short- and long-term drug assays	Low throughput and slow to produce Requires complex and expensive equipment Requires significantly more cells than other miniaturized methods Heterogeneous drug distribution across large tissues Not yet adapted to mouse hepatocyte culture
Perfused liver cultures[63–65]	Dynamic fluid flow for nutrient and waste exchange Several commercial devices available for cell culture and perfusion in single-chamber or multichamber device designs Multiple tissue models can be coupled to create "body-on-a-chip" platform Oxygen and hormone gradients can be created Maintain liver functions for several weeks	Potential binding of drugs to tubing and materials used Large dead volume requiring higher quantities of novel compounds for the treatment of cell cultures May wash away built-up beneficial molecules to cells Currently low throughput and require specialized fluid pumps and controls Not yet adapted to mouse hepatocyte culture

other aspects of liver physiology. First, while monolayers, such as in mMPCCs, allow cell visualization using standard microscopy, 3D spheroids of controlled sizes have a higher surface area-to-volume ratio to facilitate a greater level of cell–cell/cell–ECM interactions and allow assessment of cell migration in 3D, albeit high-resolution imaging in spheroids requires confocal microscopy. Nonetheless, we anticipate that mMPCCs can be adapted to 3D spheroidal models as previously done with PHH-MPCCs[59] toward allowing the highest flexibility in testing specific hypotheses. Second, future inclusion of liver NPCs and donor-matched adaptive immune cells into mMPCCs could be useful to further model liver physiology and disease; indeed, our previous work shows that the use 3T3-J2 fibroblasts to stabilize primary human hepatocytes does not prevent the investigation of pairwise interactions between the hepatocytes and liver NPCs, including Kupffer cells[27], liver sinusoidal endothelial cells[25], and hepatic stellate cells[26]. Third, incorporation of mMPCCs into perfusion-based culture devices (i.e., microfluidic tissue-on-a-chip) could allow creation of soluble factor gradients as in vivo that modulate zonated functions in hepatocytes and also enable connection of different tissue models with flowing fluid to investigate intertissue crosstalk following compound exposure; while such a configuration would significantly reduce throughput for compound testing over the use of multiwell plates, it would provide opportunities to test additional hypotheses that necessitate flow (e.g., zonation) and intertissue crosstalk (e.g., liver-produced metabolites causing toxicity or other effects in other tissue types).

In conclusion, mMPCCs sustain high levels of functions, including drug metabolism capacities, for 4 weeks, and can be used to compare strain- and species-specific hepatic responses following drug exposure. Ultimately, mMPCCs created using diverse mouse strains can be useful for elucidating a) the sensitivity of subpopulations to compound effects, b) the degree of interindividual variability in compound metabolism and toxicity, and c) the genetic determinants of compound-induced liver injury in humans.

ACKNOWLEDGMENTS: We thank Alison Bailey, Kimberly Ballinger, Dustin Berger, Matthew Davidson, Mitchell Durham, and Christine Lin for assistance with cell culture. Funding was provided by the National Science Foundation (CBET-1351909 and CBET-1706393 to S.R.K.). B.R.W., G.E.B., V.Y.S., E.L.L, and S.R.K. designed the experiments. B.R.W., G.E.B., and V.Y.S executed the experiments. B.R.W., G.E.B., and S.R.K. analyzed the data and prepared the figures. B.R.W., G.E.B., V.Y.S., E.L.L, and S.R.K. wrote and reviewed the manuscript. The authors declare no conflicts of interest.

REFERENCES

1. Olson H, Betton G, Robinson D, Thomas K, Monro A, Kolaja G, Lilly P, Sanders J, Sipes G, Bracken W, et al. Concordance of the toxicity of pharmaceuticals in humans and in animals. Regul Toxicol Pharmacol. 2000;32(1):56–67.
2. Khetani SR, Kanchagar C, Ukairo O, Krzyzewski S, Moore A, Shi J, Aoyama S, Aleo M, Will Y. Use of micropatterned cocultures to detect compounds that cause drug-induced liver injury in humans. Toxicol Sci. 2013;132(1):107–17.
3. Threadgill DW, Churchill GA. Ten years of the Collaborative Cross. Genetics 2012;190(2):291–4.
4. Kaplowitz N. Idiosyncratic drug hepatotoxicity. Nat. Rev. Drug Discov. 2005;4(6):489–99.
5. Wilkening S, Stahl F, Bader A. Comparison of primary human hepatocytes and hepatoma cell line Hepg2 with regard to their biotransformation properties. Drug Metab Dispos. 2003;31(8):1035–42.
6. Martinez SM, Bradford BU, Soldatow VY, Kosyk O, Sandot A, Witek R, Kaiser R, Stewart T, Amaral K, Freeman K, et al. Evaluation of an in vitro toxicogenetic mouse model for hepatotoxicity. Toxicol Appl Pharmacol. 2010;249(3):208–16.
7. Choi HJ, Choi D. Successful mouse hepatocyte culture with sandwich collagen gel formation. J Korean Surg Soc. 2013;84(4):202–8.
8. Meng T, Niu Y, Miao P, Ji Y, Bin P, Dai Y, Zheng Y. Optimization of primary hepatocytes model and study on the cytotoxicity of styrene and styrene oxide. J Hyg Res. 2016;45(3):367–75.
9. Guenthner CJ, Luitje ME, Pyle LA, Molyneux PC, Yu JK, Li AS, Leise TL, Harrington ME. Circadian rhythms of Per2::Luc in individual primary mouse hepatocytes and cultures. PLoS One 2014;9(2):e87573.
10. Meng Q, Tao C, Qiu Z, Akaike T, Cui F, Wang X. A hybrid substratum for primary hepatocyte culture that enhances hepatic functionality with low serum dependency. International J Nanomed. 2015;10:2313–23.
11. Desai SS, Tung JC, Zhou VX, Grenert JP, Malato Y, Rezvani M, Español-Suñer R, Willenbring H, Weaver VM, Chang TT. Physiological ranges of matrix rigidity modulate primary mouse hepatocyte function in part through hepatocyte nuclear factor 4 alpha. Hepatology 2016;64:261–75.
12. Buck LD, Inman SW, Rusyn I, Griffith LG. Co-regulation of primary mouse hepatocyte viability and function by oxygen and matrix. Biotechnol Bioeng. 2014;111(5):1018–27.
13. Miyamoto Y, Ikeuchi M, Noguchi H, Yagi T, Hayashi S. Three-dimensional in vitro hepatic constructs formed using combinatorial tapered stencil for cluster culture (TASCL) device. Cell Med. 2014;7(2):67–74.
14. Bhatia SN, Balis UJ, Yarmush ML, Toner M. Effect of cell–cell interactions in preservation of cellular phenotype: Cocultivation of hepatocytes and nonparenchymal cells. FASEB J. 1999;13(14):1883–900.
15. Bezerra JA. Liver development: A paradigm for hepatobiliary disease in later life. Semin Liver Dis. 1998;18(3):203–16.
16. Cereghini S. Liver-enriched transcription factors and hepatocyte differentiation. FASEB J. 1996;10(2):267–82.
17. Langenbach R, Malick L, Tompa A, Kuszynski C, Freed H, Huberman E. Maintenance of adult rat hepatocytes on C3H/10T1/2 cells. Cancer Res. 1979;39(9):3509–14.
18. Michalopoulos G, Russell F, Biles C. Primary cultures of hepatocytes on human fibroblasts. In Vitro 1979;15(10): 796–806.
19. Fatih N, Camberlein E, Island ML, Corlu A, Abgueguen E, Detivaud L, Leroyer P, Brissot P, Loreal O. Natural and synthetic STAT3 inhibitors reduce hepcidin expression in differentiated mouse hepatocytes expressing the

active phosphorylated STAT3 form. J Mol Med. (Berl) 2010;88(5):477–86.
20. Okada K, Ueshima S, Kawao N, Okamoto C, Matsuo K, Akao M, Seki T, Ariga T, Tanaka M, Matsuo O. Binding of plasminogen to hepatocytes isolated from injured mouse liver and nonparenchymal-cell-dependent proliferation of hepatocytes. Blood Coagul Fibrinolysis 2008; 19(6):503–11.
21. Khetani SR, Szulgit G, Del Rio JA, Barlow C, Bhatia SN. Exploring interactions between rat hepatocytes and nonparenchymal cells using gene expression profiling. Hepatology 2004;40(3):545–54.
22. Khetani SR, Chen AA, Ranscht B, Bhatia SN. T-cadherin modulates hepatocyte functions in vitro. FASEB J. 2008; 22(11):3768–75.
23. Khetani SR, Bhatia SN. Microscale culture of human liver cells for drug development. Nat Biotechnol. 2008;26(1): 120–6.
24. Hui EE, Bhatia SN. Micromechanical control of cell–cell interactions. Proc Natl Acad Sci USA 2007;104(14): 5722–6.
25. Ware BR, Durham MJ, Monckton CP, Khetani SR. A cell culture platform to maintain long-term phenotype of primary human hepatocytes and endothelial cells. Cell Mol Gastroenterol Hepatol. 2018;5(3):187–207.
26. Davidson MD, Kukla DA, Khetani SR. Microengineered cultures containing human hepatic stellate cells and hepatocytes for drug development. Integr Biol. 2017;9(8): 662–77.
27. Nguyen TV, Ukairo O, Khetani SR, McVay M, Kanchagar C, Seghezzi W, Ayanoglu G, Irrechukwu O, Evers R. Establishment of a hepatocyte–Kupffer cell coculture model for assessment of proinflammatory cytokine effects on metabolizing enzymes and drug transporters. Drug Metab Dispos. 2015;43(5):774–85.
28. Ware BR, McVay M, Sunada WY, Khetani SR. Exploring chronic drug effects on microengineered human liver cultures using global gene expression profiling. Toxicol Sci. 2017;157(2):387–98.
29. Lin C, Shi J, Moore A, Khetani SR. Prediction of drug clearance and drug–drug interactions in microscale cultures of human hepatocytes. Drug Metab Dispos. 2016;44(1): 127–36.
30. March S, Ramanan V, Trehan K, Ng S, Galstian A, Gural N, Scull MA, Shlomai A, Mota MM, Fleming HE, et al. Micropatterned coculture of primary human hepatocytes and supportive cells for the study of hepatotropic pathogens. Nat Protoc. 2015;10(12):2027–53.
31. Wang WW, Khetani SR, Krzyzewski S, Duignan DB, Obach RS. Assessment of a micropatterned hepatocyte coculture system to generate major human excretory and circulating drug metabolites. Drug Metab Dispos. 2010; 38(10):1900–5.
32. Underhill GH, Khetani SR. Bioengineered liver models for drug testing and cell differentiation studies. Cell Mol Gastroenterol Hepatol. 2018;5(3):426–39.e1.
33. Berger DR, Ware BR, Davidson MD, Allsup SR, Khetani SR. Enhancing the functional maturity of induced pluripotent stem cell-derived human hepatocytes by controlled presentation of cell–cell interactions in vitro. Hepatology 2015;61(4):1370–81.
34. Roncoroni C, Rizzi N, Brunialti E, Cali JJ, Klaubert DH, Maggi A, Ciana P. Molecular imaging of cytochrome P450 activity in mice. Pharmacol Res. 2012;65(5):531–6.
35. Cali JJ, Ma D, Sobol M, Simpson DJ, Frackman S, Good TD, Daily WJ, Liu D. Luminogenic cytochrome P450 assays. Expert Opin Drug Metab Toxicol. 2006;2(4):629–45.
36. Nelson DR, Zeldin DC, Hoffman SM, Maltais LJ, Wain HM, Nebert DW. Comparison of cytochrome P450 (CYP) genes from the mouse and human genomes, including nomenclature recommendations for genes, pseudogenes and alternative-splice variants. Pharmacogenetics 2004;14(1):1–18.
37. Jeong HG, Lee SS, Kim HK, Yang KH. Murine Cyp1a-1 induction in mouse hepatoma Hepa-1C1C7 cells by myristicin. Biochem Biophys Res Commun. 1997;233(3):619–22.
38. Donato MT, Viitala P, Rodriguez-Antona C, Lindfors A, Castell JV, Raunio H, Gomez-Lechon MJ, Pelkonen O. CYP2A5/CYP2A6 expression in mouse and human hepatocytes treated with various in vivo inducers. Drug Metab Dispos. 2000;28(11):1321–6.
39. Ukairo O, Kanchagar C, Moore A, Shi J, Gaffney J, Aoyama S, Rose KA, Krzyzewski S, McGeehan J, Andersen ME and others. Long-term stability of primary rat hepatocytes in micropatterned cocultures. J Biochem Mol Toxicol. 2013;27(3):204–12.
40. Pelkonen O, Sotaniemi EA, Ahokas JT. Coumarin 7-hydroxylase activity in human liver microsomes. Properties of the enzyme and interspecies comparisons. Br J Clin Pharmacol. 1985;19(1):59–66.
41. Prueksaritanont T, Chu X, Gibson C, Cui D, Yee KL, Ballard J, Cabalu T, Hochman J. Drug–drug interaction studies: Regulatory guidance and an industry perspective. AAPS J. 2013;15(3):629–45.
42. LeCluyse EL. Pregnane X receptor: Molecular basis for species differences in CYP3A induction by xenobiotics. Chem Biol Interac. 2001;134(3):283–9.
43. Mutoh S, Sobhany M, Moore R, Perera L, Pedersen L, Sueyoshi T, Negishi M. Phenobarbital indirectly activates the constitutive active androstane receptor (CAR) by inhibition of epidermal growth factor receptor signaling. Sci Signal. 2013;6(274):ra31.
44. Madan A, Graham RA, Carroll KM, Mudra DR, Burton LA, Krueger LA, Downey AD, Czerwinski M, Forster J, Ribadeneira MD, et al. Effects of prototypical microsomal enzyme inducers on cytochrome P450 expression in cultured human hepatocytes. Drug Metab Dispos. 2003;31(4): 421–31.
45. Shih H, Pickwell GV, Guenette DK, Bilir B, Quattrochi LC. Species differences in hepatocyte induction of CYP1A1 and CYP1A2 by omeprazole. Hum Exper Toxicol. 1999;18(2): 95–105.
46. Shiizaki K, Kawanishi M, Yagi T. Microbial metabolites of omeprazole activate murine aryl hydrocarbon receptor in vitro and in vivo. Drug Metab Dispos. 2014;42(10): 1690–7.
47. Ware BR, Berger DR, Khetani SR. Prediction of drug-induced liver injury in micropatterned co-cultures containing iPSC-derived human hepatocytes. Toxicol Sci. 2015; 145(2):252–62.
48. Xu JJ, Henstock PV, Dunn MC, Smith AR, Chabot JR, de Graaf D. Cellular imaging predictions of clinical drug-induced liver injury. Toxicol Sci. 2008;105(1):97–105.
49. Norona LM, Nguyen DG, Gerber DA, Presnell SC, LeCluyse EL. Editor's highlight: Modeling compound-induced fibrogenesis in vitro using three-dimensional bioprinted human liver tissues. Toxicol Sci. 2016;154(2):354–67.
50. Foster AJ, Chouhan B, Regan SL, Rollison H, Amberntsson S, Andersson LC, Srivastava A, Darnell M, Cairns J, Lazic

SE, et al. Integrated in vitro models for hepatic safety and metabolism: Evaluation of a human Liver-Chip and liver spheroid. Arch Toxicol. 2019;93(4):1021–37.
51. Sancheti PM, Pawar SP. In vivo toxicity evaluation of troglitazone, rosiglitazone, and pioglitazone in CD-1 Mice. Int J Pharm Biol Sci. 2016;6(1):8–15.
52. Lee YH, Chung MCM, Lin Q, Boelsterli UA. Troglitazone-induced hepatic mitochondrial proteome expression dynamics in heterozygous Sod2(+/-) mice: Two-stage oxidative injury. Toxicol Appl Pharmacol. 2008;231:43–51.
53. Ong MM, Latchoumycandane C, Boelsterli UA. Troglitazone-induced hepatic necrosis in an animal model of silent genetic mitochondrial abnormalities. Toxicol Sci. 2007; 97(1):205–13.
54. McKenzie R, Fried MW, Sallie R, Conjeevaram H, Di Bisceglie AM, Park Y, Savarese B, Kleiner D, Tsokos M, Luciano C, et al. Hepatic failure and lactic acidosis due to fialuridine (FIAU), an investigational nucleoside analogue for chronic hepatitis B. New Engl J Med. 1995;333(17): 1099–105.
55. Schmid R. Fialuridine toxicity. Hepatology 1997;25(6): 1548.
56. Gural N, Mancio-Silva L, Miller AB, Galstian A, Butty VL, Levine SS, Patrapuvich R, Desai SP, Mikolajczak SA, Kappe SHI, et al. In vitro culture, drug sensitivity, and transcriptome of plasmodium vivax hypnozoites. Cell Host Microbe 2018;23(3):395–406 e4.
57. Ballard TE, Wang S, Cox LM, Moen MA, Krzyzewski S, Ukairo O, Obach RS. Application of a micropatterned cocultured hepatocyte system to predict preclinical and human-specific drug metabolism. Drug Metab Dispos. 2016;44(2): 172–9.
58. Aleo MD, Ukairo O, Moore A, Irrechukwu O, Potter DM, Schneider RP. Liver safety evaluation of endothelin receptor antagonists using HepatoPac((R)): A single model impact assessment on hepatocellular health, function and bile acid disposition. J Appl Toxicol. 2019;39(8):1192–207.
59. Chen AA, Thomas DK, Ong LL, Schwartz RE, Golub TR, Bhatia SN. Humanized mice with ectopic artificial liver tissues. Proc Natl Acad Sci USA 2011;108(29):11842–7.
60. Ingelman-Sundberg M, Lauschke VM. Human liver spheroids in chemically defined conditions for studies of gene–drug, drug–drug and disease–drug interactions. Pharmacogenomics 2018; 19(14):1133–8.
61. Bell CC, Hendriks DFG, Moro SML, Ellis E, Walsh J, Renblom A, Fredriksson Puigvert L, Dankers ACA, Jacobs F, Snoeys J, et al. Characterization of primary human hepatocyte spheroids as a model system for drug-induced liver injury, liver function and disease. Sci Rep. 2016;6:25187.
62. Norona LM, Nguyen DG, Gerber DA, Presnell SC, LeCluyse EL. Modeling compound-induced fibrogenesis in vitro using three-dimensional bioprinted human liver tissues. Toxicol Sci. 2016;154(2):354–67.
63. Powers MJ, Janigian DM, Wack KE, Baker CS, Beer Stolz D, Griffith LG. Functional behavior of primary rat liver cells in a three-dimensional perfused microarray bioreactor. Tissue Eng. 2002;8(3):499–513.
64. Kane BJ, Zinner MJ, Yarmush ML, Toner M. Liver-specific functional studies in a microfluidic array of primary mammalian hepatocytes. Analyt Chem. 2006;78(13):4291–8.
65. Novik E, Maguire TJ, Chao P, Cheng KC, Yarmush ML. A microfluidic hepatic coculture platform for cell-based drug metabolism studies. Biochem Pharmacol. 2010; 79(7):1036–44.